Aalto University

OPEN ACCESS

This is an electronic reprint of the original article.
This reprint may differ from the original in pagination and typographic detail.

Giedraityte, Z.; Johansson, L. S.; Karppinen, M.

ALD/MLD fabrication of luminescent Eu-organic hybrid thin films using different aromatic carboxylic acid components with N and O donors

Published in:
RSC Advances

DOI:
10.1039/c6ra24175a

Published: 01/01/2016

Document Version
Peer reviewed version

Published under the following license:
Unspecified

Please cite the original version:
Giedraityte, Z., Johansson, L. S., & Karppinen, M. (2016). ALD/MLD fabrication of luminescent Eu-organic hybrid thin films using different aromatic carboxylic acid components with N and O donors. *RSC Advances*, *6*(105), 103412-103417. https://doi.org/10.1039/c6ra24175a

This material is protected by copyright and other intellectual property rights, and duplication or sale of all or part of any of the repository collections is not permitted, except that material may be duplicated by you for your research use or educational purposes in electronic or print form. You must obtain permission for any other use. Electronic or print copies may not be offered, whether for sale or otherwise to anyone who is not an authorised user.

Please do not adjust margins

RSC Advances

COMMUNICATION

ALD/MLD fabrication of luminescent Eu-organic hybrid thin films using different aromatic carboxylic acid components with N and O donors

Received 00th January 20xx,
Accepted 00th January 20xx

DOI: 10.1039/x0xx00000x

www.rsc.org/

Z. Giedraityte, L.-S. Johansson and M. Karppinen*

Atomic/molecular layer deposition (ALD/MLD) processes based on $Eu(thd)_3$ and three different aromatic organic acids with O and N donors as precursors are systematically investigated for the growth of Eu-based inorganic-organic thin-film phosphors. For all the acid precursors evaluated, i.e. 1-4-dicarboxylic, 3,5-pyridinedicarboxylic and 2,6-pyridinedicarboxylic acids, conditions are found to produce high-quality hybrid thin films through self-saturating gas-solid reactions as expected for an ideal ALD/MLD process. The resultant Eu-organic thin films show intense red photoluminescence. The luminescence characteristics depend on the manner the organic ligands are bound to Eu^{3+}; this is discussed based on FTIR, XPS, UV-vis and fluoroscence spectroscopy data measured for the films.

With the rapid advances in a number of emerging application possibilities in photonics ranging from OLEDs to bio-imaging, lanthanide-based inorganic-organic hybrid materials have become an increasingly interesting material family.[1-4] The peculiar photoluminescence characteristics of these materials such as sharp emission lines, large Stokes shifts and long lifetimes originate from the parity and spin-forbidden lanthanide ion 4f-4f transitions. Trivalent lanthanide ions alone show extremely inefficient direct photoexcitation; the function of the organic component in the hybrid is to absorb light in the UV/visible spectral range and then transfer the energy to the lanthanide ions thus sensitizing the characteristic lanthanide luminescence. The efficiency of the process varies with the nature of the ligand and the bonding between the ligand and the lanthanide ion. Polydentate pyridine carboxylates are particularly promising candidates as sensitizers:[5-7] the large lanthanide ions act as hard acids and form strong bonds with ligands having O and N donor atoms such that the resultant hybrids usually exhibit not only high thermal stabilities but also intense photoluminescence.

Department of Chemistry, Aalto University, P.O. Box 16100, FI-00076 Aalto, Finland.
E-mail: maarit.karppinen@aalto.fi

For many of the frontier applications of lanthanide-based inorganic-organic phosphors, the demand is for high-quality thin films that would moreover be e.g. transparent and flexible; also desired is that these coatings could be homogeneously deposited on various 3D surface architectures. The strongly emerging atomic/molecular layer deposition (ALD/MLD) thin-film technique[8-12] based on sequential gas-surface reactions of gaseous inorganic and organic precursors would be ultimately suited to fabricate such state-of-the-art hybrid materials. There is a strive to extend the technique to a wider range of metal and organic backbone constituents,[13-15] and recently we indeed presented a highly viable ALD/MLD process based on $Eu(thd)_3$ and 3,5-pyridinedicarboxylic acid (3,5-PDC) precursors to fabricate Eu-based inorganic-organic hybrid thin films with attractive photoluminescence properties.[16] Here upon the film growth $Eu(thd)_3$ reacts through ligand-exchange reactions with 3,5-PDC to form Eu-PDC films in an atomic/molecular layer-by-layer manner. The underlining surface reactions were shown to be self-limiting, thus providing a means to deposit precisely-thickness-controlled and conformal coatings in an atomic/molecular layer-by-layer manner over various substrate materials. We foresee that the ALD/MLD-grown Eu-hybrid thin films could be exciting new phosphor materials in applications where ultrathin luminescent coatings on flexible and/or nanostructured surfaces are needed. To gain deeper understanding of the chemical factors controlling the ALD/MLD growth and the resultant structural and luminescence properties of the Eu-hybrid films, we in this work evaluate three different aromatic dicarboxylic acids with or without pyridinic nitrogen, that is, 1,4-dicarboxylic (1,4-BDC), 3,5-pyridine-dicarboxylic (3,5-PDC) and 2,6-pyridinedicarboxylic (2,6-PDC) acids, for the ALD/MLD fabrication of Eu-hybrid phosphors.

We first investigated the film growth at different temperatures for the selected organic precursors together with $Eu(thd)_3$ as the inorganic precursor (see Fig. 1). In Fig. 2 (upper left panel) the growth-per-cycle (GPC) values achieved at different deposition temperatures are displayed as calculated

This journal is © The Royal Society of Chemistry 20xx

Please do not adjust margins

Please do not adjust margins

from the resultant film thickness values determined from the XRR data. It is seen that the GPC decreases with increasing deposition temperature for all the three processes; this is a rather typical feature for the inorganic-organic hybrid thin films grown by the ALD/MLD technique.[10,11] Even though the trend of decreasing GPC with increasing deposition temperature is very similar for the three processes, the GPC values are not exactly the same. Among the three processes the highest GPC values within the whole temperature range are for the $Eu(thd)_3$+3,5-PDC process, while the lowest values are for the $Eu(thd)_3$+2,6-PDC process; the GPC values for the $Eu(thd)_3$+1,4-BDC process are in between those for the two pyridinedicarboxylic acid based processes. The reason for the slight differences in the GPC values among the three processes should thus be in the geometrical arrangement of the functional groups rather than the nature of the functional groups, see also our discussion later on. Despite the somewhat different growth rates all the three processes yielded smooth and seemingly homogeneous films within the entire deposition temperature range studied. For the rest of the experiments we decided to concentrate on the temperature window 280-300 °C where we obtained intermediate GPC values for all the three processes.

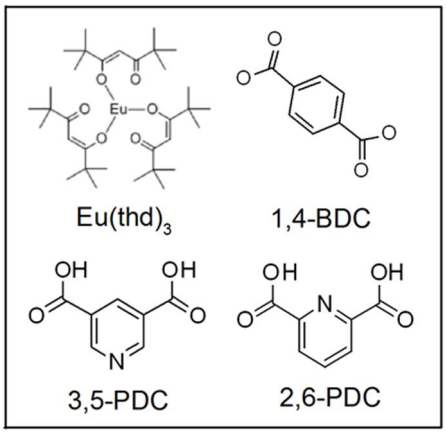

Figure 1. Precursors employed in the present study: tris(2,2,6,6-tetramethyl-3,5-heptanedionato)europium(III) ($Eu(thd)_3$), 1,4-dicarboxylic acid (1,4-BDC), 3,5-pyrdinedicarboxylic acid (3,5-PDC) and 2,6-pyridienedicarboxylic acid (2,6-PDC).

Next we confirmed the self-saturative nature of the surface reactions involved for our $Eu(thd)_3$+1,4-BDC, $Eu(thd)_3$+3,5-PDC and $Eu(thd)_3$+2,6-PDC processes by changing the precursor pulse lengths one at the time in each process and monitoring the resultant GPC values. In these experiments the precursor pulse length was fixed at 1 s for $Eu(thd)_3$ when the pulse length of the organic precursor was varied from 1 to 4 s, and at 2 s for the organic precursor pulse when the $Eu(thd)_3$ pulse length was varied from 1 to 4 s. In each experiment the purging time was always twice the pulse length of the corresponding precursor. In Fig. 2 (lower panels), we show the results obtained at 280 °C for the $Eu(thd)_3$+1,4-BDC process and at 300 °C for the $Eu(thd)_3$+3,5-PDC and $Eu(thd)_3$+2,6-PDC processes. The film growth apparently saturates even for the shortest precursor pulse lengths employed as no changes in the GPC value were seen when the pulse lengths were increased. It should be noted that we obtained similar results at all other deposition temperatures more randomly tested (data not shown here).

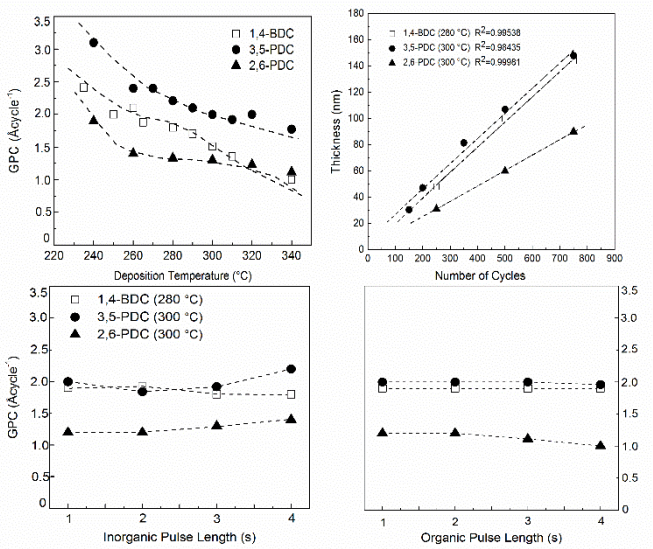

Figure 2. *Upper left*: growth per cycle (GPC) at different deposition temperatures for the three ALD/MLD processes, $Eu(thd)_3$+1,4-BDC, $Eu(thd)_3$+3,5-PDC and $Eu(thd)_3$+2,6-PDC. *Upper right*: film thickness as a function of number of deposition cycles for films deposited at 280 °C ($Eu(thd)_3$+1,4-BDC) or 300 °C ($Eu(thd)_3$+3,5-PDC and $Eu(thd)_3$+2,6-PDC). *Lower panels*: GPC as a function of the $Eu(thd)_3$ and organic precursor (1,4-BDC, 3,5-PDC or 2,6-PDC) pulse lengths for the three ALD/MLD processes; the pulse/purge lengths for the other precursor were fixed to 1 s/2 s for $Eu(thd)_3$ and to 2 s/4 s for the organic precursor.

For the rest of the experiments we selected the following pulse/purge lengths: 1 s $Eu(thd)_3$ / 2 s N_2 / 2 s organic precursor / 4 s N_2. Using these pulse lengths we then confirmed that the film thickness increased in a linear manner with increasing number of deposition cycles, see Fig. 2 (upper right panel); this is an important characteristics expected for an ideal ALD/MLD process. From the GIXRD data (not shown here) all the films were completely amorphous within the detection limit of our equipment, except one 200-nm thick film deposited from the $Eu(thd)_3$ and 1,4-BDC precursors at 300 °C; for this film one broad diffraction peak was seen at $2\theta \approx 9.25°$, corresponding to a d value of ca. 9.6 Å.

In Fig. 3 we show FTIR spectra for ca. 100-nm thick films of Eu–1,4-BDC, Eu–3,5-PDC and Eu–2,6-PDC (all deposited at 300 °C) together with the spectra for the corresponding carboxylic acid precursors for comparison; the characteristic features seen in the spectra are also summarized in Table 1. First of all, the characteristic peaks for symmetric $\nu_s(C{=}O)$ and asymmetric $\nu_{as}(COO^-)$ stretching vibrations observed for the Eu-hybrid films around 1386–1395 cm^{-1} and 1543–1584 cm^{-1}, respectively, confirm the presence of the carboxylate species in the films, while the absence of the broad absorption band around 2900–3400 cm^{-1} confirms that the films are devoid of O-H and N-H bonds, as expected. Another indication that the intended reaction indeed has taken place between the carboxylate ligands and the Eu^{3+} cation and that there is no traces of the organic precursor left in the films is the absence of the ca. 1700 cm^{-1} feature (characteristic for carboxylic acids) in the spectra for our hybrid thin films.

 This journal is © The Royal Society of Chemistry 20xx

Please do not adjust margins

Please do not adjust margins

As for the more detailed information of the bonding in the films, we should firstly look at the difference in the positions of the asymmetric and symmetric stretching vibrations of the carboxylate group as it indicates the coordination mode (see Table 1), i.e. unidentate ($\Delta v > 200$ cm^{-1}), bidentate ($50 < \Delta v < 150$ cm^{-1}) or bridging ($130 < \Delta v < 200$ cm^{-1}) type.[17] From Table 1, this difference is in the range of 165-194 cm^{-1} for Eu–3,5-PDC and Eu–2,6-PDC indicating bridging-type bonding to two different Eu atoms, while being of the border-line value (148 cm^{-1}) between those of bidentate and bridging modes for Eu–1,4-BDC. Finally the shift seen in the position of the *v*(C=N) band to lower wavenumbers, i.e. from ca. 1690 cm^{-1} for the pyridinedi-carboxylic acid precursors to ca. 1440 cm^{-1} for the Eu–3,5-PDC and Eu–2,6-PDC films, can be interpreted as an indication of the pyridine-N-coordination to the Eu^{3+} cation in our PDC-based hybrid thin films.[18-20] Hence, we may conclude that our FTIR data suggest that europium bonds to the organic precursor via nitrogen atom (if available) and two oxygen atoms but not necessarily in exactly the same way in all the three hybrid films.

Table 1. Assignment of the spectral features in the FTIR spectra.

Sample	ν(C=N) [cm^{-1}]	ν_{as}(COO$^-$) [cm^{-1}]	ν_s(COO$^-$) [cm^{-1}]	Δν(COO$^-$) [cm^{-1}]
1,4-BDC	-			
Eu–1,4-BDC	-	1543	1395	148
3,5-PDC	1690			
Eu–3,5-PDC	1602, 1442	1551	1386	165
2,6-PDC	1690			
Eu–2,6-PDC	1616, 1438	1584	1390	194

The FTIR results are further supported by the XPS data recorded for the three hybrid thin films and the corresponding organic precursors for reference, see Fig. 4. From the wide-energy-range spectra (left panel) it can be confirmed that the sample surfaces consist of carbon, oxygen, nitrogen and europium only (the latter one in the films only), as expected. From the high-resolution spectra for carbon, oxygen, nitrogen and europium, the main peaks seen at ca. 285 and 289.2 eV for carbon atoms in aromatic ring and carbonylic group, respectively, at 532 eV for oxygen in carbonylic group, at ca. 399 eV for pyridinic nitrogen and at 137 eV for strongly-coordinated europium all fit well with the relevant reference data.[21,22]

The more detailed XPS analysis reveals that upon the hybrid film deposition the binding energies of the N atoms of the pyridine ring change upon the film formation confirming that Eu indeed bonds also to nitrogen in both Eu–3,5-PDC and Eu–2,6-PDC. Another indication of this is that also the binding energies of the aromatic carbon atoms (compared to the values in the precursors) somewhat change for the PDC-based films.[23]

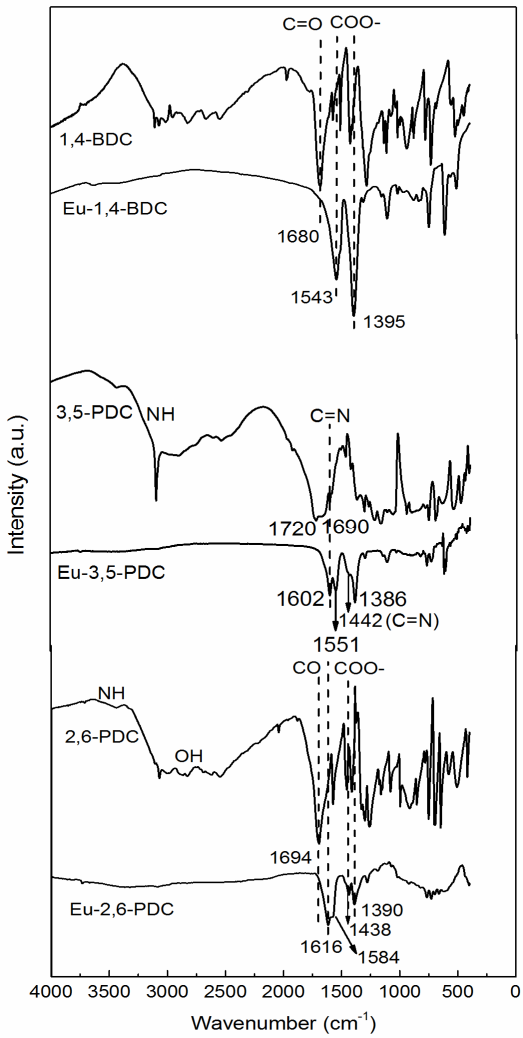

Figure 3. FTIR spectra for the hybrid thin films, Eu–1,4-BDC, Eu–3,5-PDC and Eu–2,6-PDC, and the corresponding organic precursors.

Please do not adjust margins

Please do not adjust margins

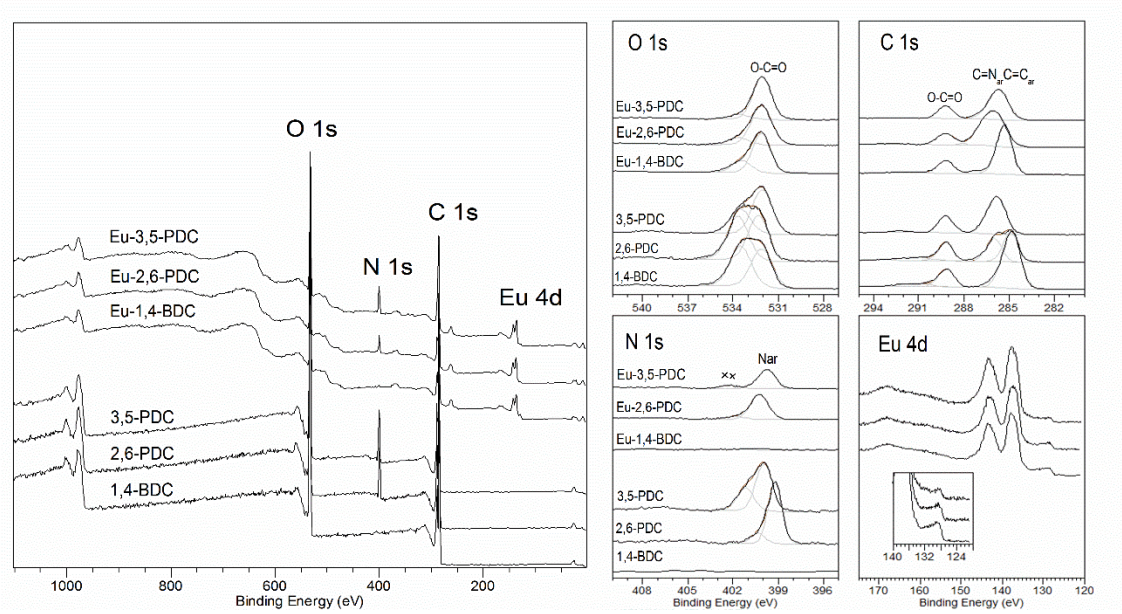

Figure 4. XPS spectra for the hybrid thin films, Eu–1,4-BDC, Eu–3,5-PDC and Eu–2,6-PDC, and the corresponding organic precursors.

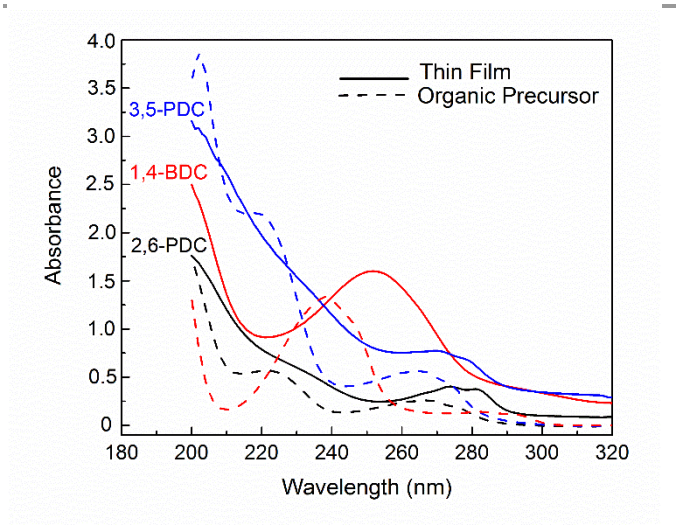

Figure 5. UV-vis spectra for the hybrid thin films, Eu–1,4-BDC, Eu–3,5-PDC and Eu–2,6-PDC, and the corresponding organic precursors (dissolved in ethanol).

The three hybrid thin films and their organic precursors were also investigated using UV-vis absorption spectroscopy, see Fig. 5. The π-π* bands seen in the spectra are attributed to intra-ligand transitions in the UV region and to MLTC (metal-to-ligand charge transfer) transition in the visible region.[24-25] When the organic molecule binds to a metal atom, a shift in the π-π* transition is expected. This is seen for all the three precursor/hybrid film pairs. Moreover seen from Fig. 5 is the fact that the two PDC-based Eu–2,6-PDC and Eu–3,5-PDC hybrid films possess an absorption band around 270 nm, which in contrast is missing for the Eu–1,4-BDC film (having a band with the maximum around 250 nm).

In Fig. 6 we display the photoluminescence excitation and emission spectra for the three hybrid Eu-organic thin films. Firstly, the excitation spectra monitored at the characteristic 615-nm Eu^{3+} emission due to the $^5D_0$-$^7F_2$ transition reveal efficient energy transfer from the organic component to the Eu^{3+} cations in all the three cases; note that the organic molecules possess an absorption band in the UV region due to the π-π* transitions. The most interesting observation is that whereas the Eu–1,4-BDC film exhibits a single excitation band around 250 nm, the two PDC-based films possess an additional lower energy excitation band around 270 nm which corresponds to the HOMO-LUMO absorption transition of pyridine molecules.[26] The fact that the maximum of the excitation band lies above 250 nm for Eu–2,6-PDC and Eu–3,5-PDC means that the light conversion process involves an efficient multiphoton assistance. The luminescence emission spectra show the same characteristic Eu^{3+} emission lines corresponding to the $^5D_0$-^7F_J (J=0-4) transitions for all the three thin films. However, Eu–3,5-PDC has the highest 615 nm/590 nm intensity (or area) ratio when compared with the rest of the hybrids, favouring the red emitted colour (Fig. 6). In general, it can be concluded that all our three-types of Eu-based inorganic-organic hybrid thin films are efficient red phosphors the optimal excitation wavelength depending on the composition of the organic antenna.

Finally, we like to emphasize that our Eu-hybrid films are chemically and thermally extremely stable under ambient conditions. This was confirmed with repeated XRR, FTIR and photoluminescence measurements after the storage of the films in ambient air at room temperature up to periods extending to a year and also upon annealing in air up to 500 °C.

This journal is © The Royal Society of Chemistry 20xx

Please do not adjust margins

Please do not adjust margins

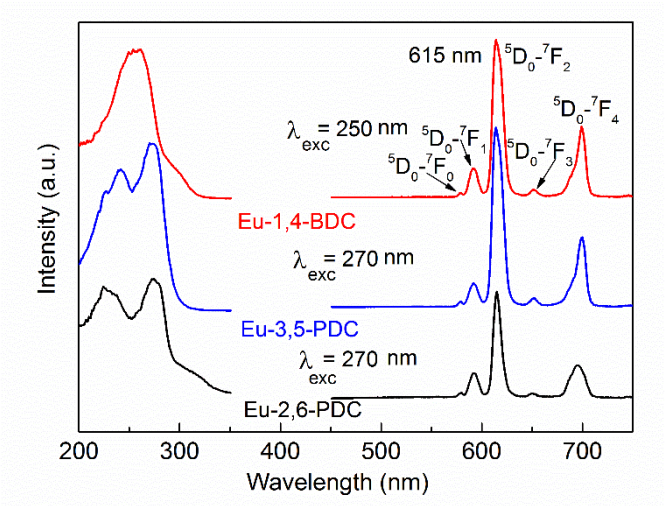

Figure 6. Photoluminescence excitation and emission spectra for the hybrid thin films, Eu–1,4-BDC, Eu–3,5-PDC and Eu–2,6-PDC.

Experimental section

The ALD/MLD fabrication of the hybrid Eu-organic thin films was performed in a commercial ALD reactor (ASM Microchemistry Ltd.) using the following precursors: $Eu(thd)_3$ (thd: 2,2,6,6-tetramethyl-3,5-heptanedione) prepared in-house, 1,4-bicarboxylic acid (1,4-BDC; TCI Europe N.V.), 3,5-pyridinedicarboxylic acid (3,5-PDC; TCI Europe N.V.) and 2,6-pyridinedicarboxylic acid (2,6-PDC; Sigma Aldrich); for the structures of the precursors, see Fig. 1. During the depositions, the precursor powders were kept in glass crucibles inside the reactor, $Eu(thd)_3$ at 140 °C and the organic precursors at 212 °C (1,4-BDC) or 235 °C (3,5-PDC and 2,6-PDC). These precursor sublimation temperatures were optimized in our preliminary experiments; see also Ref. 16. Due to the high volatility of the organic precursors, the crucible containing the organic precursor was covered with quartz glass wool (Nabertherm). Nitrogen (>99.999%; Schmidilin UHPN 3000 N_2 generator) was used as a carrier and purging gas, and a pressure of 2 to 4 mbar was maintained in the reactor during the film depositions. The following pulse/purge lengths were used for most of the experiments: 1 s $Eu(thd)_3$ / 2 s N_2 / 2 s organic precursor (1,4-BDC, 3,5-PDC or 2,6-PDC) / 4 s N_2. The film growth was investigated in the deposition temperature range from 240 to 340 °C. The depositions were performed on quartz and/or p-type Si(100) (Okmetic Ltd.) substrates cut to ca 3.5 x 3.5 cm^2 pieces.

The film thicknesses and densities were determined with X-ray reflectivity (XRR; PANalytical X'Pert MPD Pro Alfa 1). The XRR data were fitted using (X'Pert HighScore Plus) Reflectivity software. The thickness values were obtained using the Fourier method. Grazing-incident X-ray diffraction measurements (GIXRD; X'Pert MPD PRO Alfa 1, PANanalytical; Cu-Kα radiation) were carried out to investigate the crystallinity of the samples. Fourier-transform infrared spectroscopy (FTIR; Nicole Magna 750) was used to identify the organic components in the samples. The measurement chamber was purged with dry air, and the spectrum measured for the substrate was subtracted from those for the thin-film samples. The surface chemical composition of the films was quantified by means of X-ray photoelectron spectroscopy (XPS; AXIS Ultra, Kratos Analytical, Manchester, U.K.) with monochromated Al Kα X-ray source and charge neutralisation utilising slow, thermal electrons. All samples were measured as-received but pre-evacuated overnight in order to obtain stable ultrahigh vacuum (UHV) conditions, and a pure cellulose specimen was used as the in-situ reference during the measurements. The binding energies were corrected using the high-resolution data from C 1s and N 1s, according to Beamson and Briggs value for aliphatic carbon atoms at 285.0 eV,[21] and expecting similar binding energy for the well resolved carboxylic component in C 1s (at 289.2 eV) in all samples.

Finally the films were characterized for their optical properties. UV-visible absorption spectra were recorded using Perkin Elmer Lambda 950 UV/Vis/NIR absorption spectrophotometer. For the photoluminescence characteristics we collected both excitation (250 – 350 nm; λ_{em} = 615 nm) and emission (450 – 750 nm; λ_{exc} = 250 – 270 nm) spectra using QuantaMaster 40 spectrofluorometer from Photon Technology International. A front-face setup at an angle that minimized the reflected and scattered light from the sample (30~40 degs.) was used. The second order peaks were eliminated by using a 400-nm long pass filter (FGL400, Thorlabs) in the emission channel; the emission and excitation slits used in the measurements were set to 3 nm and the fluorescence spectra were corrected using the instrument's excitation and emission corrections provided by the manufacturer. Our Quantar Master 40 spectrofluorometer does not allow the use of excitation wavelengths below 250 nm. Hence we additionally measured the excitation spectra with Perkin Elmer Spectrometer (LS5OB Model using 515 cut-off filter); the low-wavelength area of the given excitation spectra are from these measurements.

Conclusions

Three different dicarboxylic acid molecules were examined together as potential organic precursors for ALD/MLD processes to be combined with europium for efficient thin-film phosphors. Two of the molecules (pyridine-2,5-dicarboxylic acid and pyridine-2,6-dicarboxylic acid) contained pyridine-type nitrogen while the third molecule (1,4-dicarboxylic acid) had no nitrogen atoms. All the three different organic precursors yielded high-quality hybrid Eu-organic thin films; the growth rates were somewhat different though, presumably due to the different precursor geometries. From FTIR and XPS spectra it was revealed that Eu binds to both the pyridinic N atoms (if available) and the carboxylic O atoms, but the coordination may not occur in an exactly same way in all the three different films. The highest growth rates were achieved at all the deposition temperatures for Eu–3,5-PDC and Eu–1,4-BDC.

All our three-types of Eu-based inorganic-organic hybrid thin films appeared as efficient red phosphors. In particular, the presence of the bidentate nitrogen donor ligands was found to extend the photoluminescence excitation wavelength range to

This journal is © The Royal Society of Chemistry 20xx

Please do not adjust margins

Please do not adjust margins

the higher wavelengths. We believe that our new ALD/MLD grown highly stable Eu-organic hybrid thin films are potential candidates for various future applications in photonics.

Acknowledgment

The present work has received funding from the European Research Council under the European Union's Seventh Framework Programme (FP/2007-2013)/ERC Advanced Grant Agreement (No. 339478). Dr. Joseph Campbell is acknowledged for performing the XPS experiments.

Notes and references

1 K. Binnemans, *Chem. Rev*., 2009, 109, 4283-4374.
2 L. D. Carlos, R. A. S. Ferreira, V. de Z. Bermudez, B. J. Lopez and P. Escribano, *Chem. Soc. Rev.*, 2011, 40, 536-549
3 B. Yan, *RSC Adv.*, 2012, 2, 9304-9324.
4 C. Zhang and J. Lin, *Chem. Soc. Rev*., 2012, 41,7938-7961
5 V. T. Freitas, L. Fu, A. M. Cojocariu, X. Cattoën, J. R. Bartlett, R. Le Parc, J.-L. Bantignies, M. W. C. Man, P. S. André, R. A. S. Ferreira and L. D. Carlos, *Appl. Mater. Interfaces*, 2015, 7, 8770-8778.
6 C. Tao, K. Du, Q. Yin, J. Zhu, H. Yan, F. Zhu and L. Zhang, *RSC. Adv.,* 2015, 5, 58936-58942.
7 S. D. Petro, D. Imbert and M. Mazzanti, *Chem. Commun*., 2014, 50, 10323-10326.
8 O. Nilsen, K. B. Klepper, H. Nielsen and H. Fjellvåg, *ECS Trans*., 2008, 16, 3–14.
9 K. B. Klepper, O. Nilsen and H. Fjellvåg, *Dalton Trans*., 2010, 39, 11628-11635.
10 S.M. George, *Chem. Rev*., 2010, 110, 111-31.
11 A. Sood, P. Sundberg, J. Malm and M. Karppinen, *Appl. Surf. Sci*., 2011, 257, 6435-6439.
12 P. Sundberg and M. Karppinen, *Beilstein J. Nanotechnol*., 2014, 5, 1104-1136.
13 A. Tanskanen and M. Karppinen, *Dalton Trans*., 2015, 44, 19194-19199.
14 E. Ahvenniemi and M. Karppinen, *Chem. Commun*., 2016, 52, 1139-1142.
15 M. Nisula and M. Karppinen, *Nano Lett*., 2016, 16, 1276-1281.
16 Z. Giedraityte, P. Sundberg and M. Karppinen, *J. Mater. Chem. C*, 2015, 3, 12316-12321.
17 K. B. Klepper, O. Nilsen, S. Francis and H. Fjellvåg, *Dalton Trans.*, 2014, 43, 3492-3500.
18 H. Xiao, M. Chen, C. Mei, H. Yin, X. Zhang and X. Cao, *Spectrochim. Acta*, 2011, A84, 238-242.
19 S. Raphael, M. L. P. Reddy, K. V. Vasudevan and A. H. Cowley, *Dalton Trans.,* 2012, 41, 14671-14682.
20 L. Wasylina, E. Kucharska, Z. Weglinski and A. Puszko, Chem. Heterocycl. Compd., 1999, 35, 186-194.
21 G. Beamson and D. Briggs: High resolution XPS of Organic Polymers. The Scienta ESCA3000 Database. Wiley, Chichester, 1992.
22 J. Chastain and R. G. King Jr (eds): Handbook of X-Ray Photoelectron Spectroscopy. Physical Electronics Inc., 1995 Eden Prairie.
23 G. Paolucci, R. D'Ippolito, C. Ye, C. Qian, J. Gräper and D.R. Fischer, *J. Organomet. Chem.*, 1994, 471, 97-104.
24 J.-M. Siaugue, F. S.-Dioury, A. F.-Reguillon, V. Wintgens, C. Madic, J. Foos, A. Guy, *J. Photochem. Photobiol.,* 2003, 156, 23-29.
25 J.-C. G. Bünzli and S. V. Eliseeva, Comprehensive Inorganic Chemistry II: From Elements to Applications, 2013, 8, 339–398.
26 C. Truillet, F. Lux, T. Brichart, G. W. Lu, Q. H. Gong, J. Appl. Phys. Lett., 2013, 114, 114308.

 This journal is © The Royal Society of Chemistry 20xx

Please do not adjust margins